

Coherently photo-induced ferromagnetism in diluted magnetic semiconductors

J. Fernández-Rossier,^{1,2*} C. Piermarocchi^{3,4}, P. Chen^{3,5}, A. H. MacDonald¹ and L. J. Sham³

¹ *Department of Physics, University of Texas at Austin. University Station C1600, Austin, TX 78712*

² *Departamento de Física Aplicada, Universidad de Alicante, San Vicente del Raspeig 03690, Alicante, Spain*

³ *Department of Physics, University of California San Diego. 9500 Gilman Drive, La Jolla, CA 92093*

⁴ *Department of Physics and Astronomy Michigan State University. 4263 Biomedical and Physical Sciences East Lansing, MI 48824-2320*

⁵ *Department of Chemistry University of California Berkeley. 406 Latimer Hall, Berkeley, CA 94720-1460*

(Dated: June 19, 2018)

Abstract

Ferromagnetism is predicted in undoped diluted magnetic semiconductors illuminated by intense *sub-bandgap* laser radiation. The mechanism for photo-induced ferromagnetism is coherence between conduction and valence bands induced by the light which leads to an optical exchange interaction. The ferromagnetic critical temperature T_C depends both on the properties of the material and on the frequency and intensity of the laser and could be above 1K.

PACS numbers:

Information processing in electronic devices is based on control of charge flow in semiconductor materials, whereas non-volatile information storage exploits ferromagnetism, spontaneous alignment of the spins of many electrons. *Spintronics*¹ aims to achieve a merger of these technologies, motivating interest in new ferromagnetic semiconductors like (Ga,Mn)As and other (III,Mn)V compounds², and in diluted magnetic semiconductors (DMS) like (Cd,Mn)Te and other (II,Mn)VI materials³ with free moments that can be aligned by external fields. The optical properties of these semiconductors are particularly interesting in this respect, because laser radiation can control both charge and spin dynamics⁴. The possibility of optically controlling semiconductors with dilute magnetic elements is now being explored actively⁵.

In this paper we predict a qualitatively new effect, photo-induced ferromagnetism, in which magnetic order is induced in an otherwise paramagnetic (II,Mn)VI DMS by laser light that is *below* the absorption edge. The influence of the laser field on the electronic system is reactive, rather than dissipative and follows ultimately from a change in the effective electronic Hamiltonian analogous to those that yield dipole forces in atomic physics. The II-VI parent compounds are intrinsic semiconductors with states of *p* character at the top of the valence band and of *s* character at the bottom of the conduction band⁶. They have a sizable interband optical matrix element, $\vec{d}_{cv} = \langle v | e\vec{r} | c \rangle$. In (II,Mn)VI alloys, Mn substitutes for the group-II atoms. The electronic structure of the external *s, p* shells of Mn and group II atoms is very similar, so that the conduction and valence band are barely affected by moderate Mn doping. However, the *d* shell of each Mn atom is only half full, in contrast to the full shells of the atoms for which they substitute, and forms a local moment with spin $S = \frac{5}{2}$. These magnetic moments are the only low energy electronic degrees of freedom in ideal (II,Mn)VI materials.

The magnetic moment of a Mn *d* shell interacts with the spins of electrons in both conduction and valence bands through the exchange coupling

$$\mathcal{H}_{\text{exch}} = \sum_{i,b} J_b \vec{M}_i \cdot \vec{S}_b(\vec{R}_i), \quad (1)$$

where \vec{M}_i refers to the Mn atom located at \vec{R}_i , the spin density of the $b = e$ conduction electrons and $b = h$ valence band holes is $\vec{S}_b(\vec{R}_i)$, and J_b are the exchange coupling constants⁶. When the Mn atoms are spin-polarized this interaction leads, in a mean field and virtual crystal approximation (MFVCA) whose approximate validity is well established^{6,7}, to an

effective magnetic field $g\mu_B\vec{B}^{\text{eff}} \equiv J_{e,h}c_{\text{Mn}}\vec{\mathcal{M}}$ experienced by the spins of the carriers, where c_{Mn} is the density of Mn atoms and $\vec{\mathcal{M}}$ is their average magnetization. This leads to band spin-splittings as large as 100 meV, evident in optical spectra and known as *giant Zeeman splittings*⁶.

In doped systems band electrons mediate RKKY interactions between Mn spins. On the other hand, virtual fluctuations in the Mn valence lead to short range superexchange antiferromagnetic interactions which couple only nearest neighbors. In a sample with a fraction x of Mn randomly located at the cation sites, $x_{\text{eff}} \equiv x(1-x)^{12}$ is the fraction of sites containing Mn atoms without a magnetic first neighbor. Consequently, samples with a low Mn concentration ($x \simeq 0.01$) and no band carriers are paramagnetic.

It has been shown⁸ that two localized spins in a semiconductor can interact via the virtual carriers created in the (otherwise empty) bands by a laser of frequency smaller than the band gap. The effective interaction is a ferromagnetic Heisenberg coupling which we shall call optical RKKY (ORKKY). It is our contention that the ORKKY interaction can drive a diluted magnetic semiconductor into a ferromagnetic phase at low temperatures. In this paper, we develop a microscopic theory for this new type of ferromagnetism and we explore its properties.

When the material is illuminated by a laser with electric field E_α , and frequency ω_L below the semiconductor band gap, E_g , a reactive dipolar energy is stored in the semiconductor:

$$\mathcal{E} = - \sum_{\alpha\beta} \chi'_{\alpha\beta}(\omega_L) E_\alpha E_\beta \quad (2)$$

where $\chi'_{\alpha\beta}(\omega_L)$ is the real part of the retarded optical response function. In this case, as in many others where direct absorption processes are negligible, the laser field acts like a new tunable thermodynamic variable which changes the properties of the system. $\chi'_{\alpha\beta}(\omega)$ depends on the inter-band transition energies which, due to the exchange interaction (1), depend in turn on the collective magnetization $\vec{\mathcal{M}}$. In an illuminated sample, \mathcal{E} *does* depend on $\vec{\mathcal{M}}$. As we show below, \mathcal{E} is minimized when the Mn spins are fully polarized and the system is ferromagnetic. Importantly, because $\hbar\omega_L < E_g$, the dissipative part $\chi''_{\alpha\beta}(\omega_L)$ of the response function is zero, so that no real electron-hole pairs are created, and heating is strongly suppressed.

We now derive \mathcal{E} starting from the microscopic Hamiltonian. The relevant degrees of freedom are the electrons in the conduction band, holes in the valence band and the Mn spins.

The exchange interaction (1) is included in the VCMFA, which results in a spin splitting of the bands when the Mn spins are polarized^{6,7}. For simplicity, we have neglected the important spin-orbit interaction influence on the valence bands; although these interactions do not change the qualitative physics, they do introduce a characteristic dependence on the laser light polarization that we do not discuss here. A classical laser field couples the valence and conduction bands. We only consider here the case of unpolarized laser light, where the two optically active (OA) interband transitions are driven with equal strength. We use the selection rule for the heavy holes at $k = 0$ so that an electron with spin σ is promoted from the valence band to the conduction band. The resultant magnetization comes from the cooperative effects of the Mn spins through their interactions with the carriers, unlike optical orientation effects that can be induced by polarized light in these materials.

The Hamiltonian reads $H = H_c + H_v + H_L + V_C$ with:

$$\begin{aligned}
H_c &= \sum_{\sigma, \vec{k}} \left[\epsilon_k^e - \frac{\sigma}{2} J_e c_{Mn} |\vec{\mathcal{M}}| \right] c_{\vec{k}, \sigma}^\dagger c_{\vec{k}, \sigma} \\
H_v &= \sum_{\sigma, \vec{k}} \left[\epsilon_k^h - \frac{\sigma}{2} J_h c_{Mn} |\vec{\mathcal{M}}| \right] d_{\vec{k}, \sigma}^\dagger d_{\vec{k}, \sigma} \\
H_L &= \frac{\Omega}{2} \sum_{\vec{k}, \sigma} c_{\vec{k}, \sigma}^\dagger e^{i\omega_L t} d_{\vec{k}, \sigma}^\dagger + h.c. \\
V_C &= \frac{1}{2\mathcal{V}} \sum_{\vec{q}} V(\vec{q}) \rho(\vec{q}) \rho(-\vec{q})
\end{aligned} \tag{3}$$

where we have chosen the spin quantization axis along the collective magnetization axis $\vec{\mathcal{M}}$. The conduction and valence band dispersions are ϵ_k^e and ϵ_k^h respectively. The strength of the light matter coupling is quantified by the Rabi energy, $\Omega = d_{cv} E_0$ where E_0 is the amplitude of the electric field of the laser. The last term accounts for the Coulomb interaction in the dominant term approximation with $\rho(q) = \rho_e(q) - \rho_h(q)$, $\rho_e(q) = \sum_{\vec{k}, \sigma} c_{\vec{k}, \sigma}^\dagger c_{\vec{k}+\vec{q}, \sigma}$, $\rho_h(q) = \sum_{\vec{k}, \sigma} d_{\vec{k}, \sigma}^\dagger d_{\vec{k}+\vec{q}, \sigma}$, $V(q) = \frac{4\pi}{\epsilon q^2}$ and \mathcal{V} stands for the volume of the sample.

The dynamics of the carrier density matrix under the influence of Hamiltonian (3) in the spinless case with $J_{e,h} = 0$ has been studied previously by a number of authors, who treat Coulomb interactions in the Hartree Fock (HF) approximation^{9,10,11}. Numerical solution of the dynamical equations¹¹ show that the density matrix reaches a steady state due to the inhomogeneous broadening provided by the different k states. Spontaneous emission and other phenomena will also contribute to the damping of the density matrix dynamics in a time scale T_2 which is in the picosecond range. The HF steady state can be described as the

vacuum of a dressed Hamiltonian¹⁰ and resembles very much a BCS state for excitons, where Ω and the electron hole (eh) interaction act as the pairing force and $\delta_0 \equiv E_g - \omega_L$ plays the role of the chemical potential. When δ_0 is positive and sufficiently large, the average density of band carriers vanishes identically when the laser is switched off. In that limit, the wave function of the ground state of the dressed Hamiltonian can be mapped to a coherent state of non-interacting bosonic excitons⁹ with binding energy ϵ_x , Bohr radius a_B and ground state wave function $\psi_{1s}(r)$ corresponding to the electron hole Coulomb potential $V(q)$ above. A crossover to the incoherent region, in which the density of carriers can be non zero when the laser is switched off occurs when δ_0 decreases towards smaller or even negative values.

When the spin degree of freedom is included, the equations for the two optically active channels decouple in the HF approximation¹² for an unpolarized laser. The two sets of equations for the carrier density matrix of the two OA channels, + and -, are identical to those of the spinless case^{9,10,11} except for the detuning, which acquires a spin dependent magnetic shift. It proves useful to define a detuning renormalized by the excitonic effects, $\delta \equiv \delta_0 - \epsilon_x$ and a spin dependent detuning

$$\delta_{\pm}(\mathcal{M}) = E_g - \omega_L - \epsilon_x \pm \mathcal{J}(\mathcal{M}) \equiv \delta \pm \mathcal{J}(\mathcal{M}) \quad (4)$$

with $\mathcal{J}(\mathcal{M}) \equiv (J_h - J_e)c_{\text{Mn}} \frac{\langle \mathcal{M} \rangle}{2}$. As a result of the magnetization, the detuning in one channel increases whereas in the other it decreases. For $\mathcal{M} = 0$ the coherent region (no absorption) occurs for $\delta > 0$ ¹¹. In order to keep the semiconductor transparent in the ferromagnetic phase, we need $\delta > \mathcal{J}(\mathcal{M})$. For the DMS considered below, the magnetic shift is large enough so that the system is in the non-interacting exciton situation for which analytical results are available⁹. For instance, the density of virtual excitons in each channel reads:

$$n_{\pm} a_B^3 = \frac{1}{4\pi} \frac{\Omega^2}{(\delta_{\pm})^2} \quad (5)$$

This result is valid provided that $n_{\sigma} a_B^3 < 0.1$, which is the case for all the results presented below. This condition imposes both a lower bound for δ , which must be larger than $\delta_{\text{min}} = |\mathcal{J}(\mathcal{M} = S)| = J_{\text{max}}$, and an upper bound for Ω , which must be smaller than $\Omega_{\text{max}} = 1.12 \times (\delta - \delta_{\text{min}})$. The former is the condition for the material to remain non-absorbing in the ferromagnetic phase, whereas the latter is the limit for the validity of the independent exciton approximation. In this limit the reactive dipolar energy stored in the semiconductor

because of the interaction with the laser reads:

$$\mathcal{E}(\mathcal{M}) = -\frac{\mathcal{V}\Omega^2|\psi_{1s}(0)|^2}{4} \left[\frac{1}{\delta_+} + \frac{1}{\delta_-} \right] \quad (6)$$

which should be compared with (2). Formally eq. (6) is the ground state energy of the dressed Hamiltonian, in the non-interacting exciton limit. To explore the collective properties of the Mn magnetic moments under the influence of the laser, we assume that the magnetic degrees of freedom are in thermal equilibrium and that their internal energy \mathcal{E} is given by Eq. (6). The magnetization is determined by the competition between the dipolar energy density $\mathcal{G}_\mathcal{E} \equiv \frac{1}{\mathcal{V}} \mathcal{E}(\mathcal{M})$ and the entropy density in $\mathcal{G}_S = -c_{Mn}k_bT\mathcal{S}(\mathcal{M})$, where $\mathcal{S}(\mathcal{M})$ is the entropy per spin as a function of the magnetization¹³. When the paramagnetic to ferromagnetic phase transition is continuous, we can expand $G(\mathcal{M})$ around $\mathcal{M} = 0$ to obtain an analytical formula for the Curie Temperature:

$$k_B T_C = \frac{S(S+1)}{3} (J_e - J_h)^2 c_{Mn} \frac{|\psi_{1s}(0)|^2 \Omega^2}{4\delta^3}. \quad (7)$$

We note that the same equation can be derived from the mean field theory using the effective Heisenberg interaction defined by the optical exchange coupling derived in ref. 8. From equation (7) and the numerical evaluation of T_C shown below, we conclude that the important factors to achieve sizable Curie Temperature are compact excitons (small a_B) and large Rabi energy Ω . From this point of view, (Zn,Mn)S and (Zn,Mn)Se seem to be the most promising in the II-VI family, due to their small Bohr radii.

In figure 1 we plot $\mathcal{G}_\mathcal{E}(\mathcal{M})$ and $\mathcal{G}_S(\mathcal{M})$ for bulk $\text{Zn}_{0.988}\text{Mn}_{0.012}\text{S}$ ($x_{\text{eff}} = 0.01$) under the influence of a laser with Rabi energy $\Omega = 5$ meV and a detuning $\delta = 41$ meV¹⁴. For this concentration, the magnetic shift for the fully polarized case is $J_{\text{max}} = 21$ meV. The upper panel of figure 1-a shows $\mathcal{G}_S(\mathcal{M})$, which favours magnetic disorder ($\mathcal{M}=0$). In the middle panel of figure 1-a we see how the dipolar energy is minimized for a maximal magnetic order $M = 5/2$. In figure 1-b we plot the total Landau functional $G(\mathcal{M}) = \mathcal{G}_\mathcal{E} + \mathcal{G}_S$, for a set of temperatures between 105 and 115 mK. For each temperature, the order parameter \mathcal{M} is obtained by minimization of $G(\mathcal{M})$ (magenta points in figure 1b). The curve $\mathcal{M}(T)$ so generated is shown in the lower panel of figure 1-a. A discontinuous phase transition from paramagnetic ($\mathcal{M} = 0$) to ferromagnetic ($\mathcal{M} \neq 0$) occurs at $T_C = 114$ mK. In that panel we also show $\mathcal{M}(T)$ for some other detunings, $\delta = 26$ meV ($T_C = 778$ mK), $\delta = 71$ meV ($T_C = 22$ mK). We see that T_C is a decreasing function of δ and that the shape of the $\mathcal{M}(T/T_C)$ curve

varies: our model predicts continuous and discontinuous phase transitions in different regions of the phase diagram. Conveniently, equation (7) remains a good approximation for T_C even when the transition is discontinuous.

The Curie temperature as a function of δ and Ω is shown in figure 2-A for $\text{Zn}_{0.988}\text{Mn}_{0.012}\text{S}$. From figure 2B it is apparent that ferromagnetism can be switched on and off, at a given temperature, by adjusting the intensity or the frequency of the laser. For a laser field with Rabi energy $\Omega = 10$ meV and $\delta = 30.5$ meV our theory predicts $T_C = 1.5$ Kelvin. Continuous wave laser excitation with Rabi splitting $\Omega = 0.2$ meV has been achieved¹⁵ which would yield $T_c \simeq 50$ mK for bulk $\text{Zn}_{0.988}\text{Mn}_{0.012}\text{S}$ and $\delta = 21.6$ meV¹⁷. In the opposite limit, values of Ω as large as 1.5 eV can be achieved with 5 femtosecond laser pulses¹⁶. However, in order to observe ferromagnetic order the laser pulse must be longer than the transition switching time, which should presumably have the same order of magnitude as T_1 , the Mn longitudinal relaxation time. In the absence of laser driven interactions, this quantity depends strongly on x , the Mn concentration, indicating that the superexchange interactions are the dominant relaxation mechanism¹⁸. For $x \simeq 0.01$, the laser driven interaction is dominant and presumably as efficient as the superexchange interactions in samples with larger Mn concentrations, where T_1 can be of the order of 0.2 ns^{5,18}. In contrast, the ferromagnetic *interactions* will switch on and off as fast as the laser pulse, on a femtosecond time scale with state of the art laser techniques.

The full phase diagram in T and δ would have six distinct regimes (see figure 2C). For $\delta > J_{\text{max}}$ the semiconductor is always transparent and the system can undergo the purely coherent ferromagnetic phase transition at a T_C close to the estimates plotted in figure 2A. For $0 < \delta < J_{\text{max}}$, the system is transparent and paramagnetic at high temperature, but has the potential to become ferromagnetic and absorbing at low temperatures. In this situation, the system might return to the paramagnetic phase, because of heating, or might be ferromagnetic (due to the standard RKKY interaction mediated by the real photocarriers). Finally, for negative detuning the system is always absorbing, and photo-induced carriers can lead to ferromagnetism through the same mechanisms that apply for equilibrium carriers, leading to a transition at $k_B T_C = \frac{S(S+1)}{3} \frac{2n^{1/3} c_{\text{Mn}}}{\hbar^2 (3\pi^2)^{(2/3)}} (J_{sd}^2 m_c + J_{pd}^2 m_v)$ where n is the density of photocarriers. Ferromagnetism induced by (real) photocarriers has been observed in (Cd,Mn)Te heterostructures at 2 Kelvin¹⁹

In summary, we propose that a diluted magnetic semiconductor exposed to a laser below

the absorption threshold will undergo a ferromagnetic phase transition at low temperatures. The ferromagnetism takes place because the reactive dipolar energy induced in the semiconductor is minimized by the ferromagnetic configuration. Microscopically, the spins interact with each other via an optical RKKY interaction mediated by virtual carriers⁸. The ferromagnetic interactions are switched on and off as fast as the laser. The mechanism of this laser induced ferromagnetism relies on interband optical coherence and is radically different from other types of carrier mediated ferromagnetism.

We thank T. Dietl for fruitful discussions. This work has been supported by the Welch Foundation, the Office of Naval Research under grant N000140010951, DARPA/ONR N0014-99-1-1096, NSF DMR 0099572, DMR-0312491 and Ramón y Cajal program (MCYT). This has been partly funded by FEDER funds. Ministerio de Ciencia y Tecnología, MAT2003-08109-C02-01.

-
- ¹ S. A. Wolff *et al* Science **294** 1488 (2001). D. D. Awschalom, D. Loss and N. Samarth, Ed, *Semiconductor Spintronics and Quantum Computation* , (Springer, New York, 2002).
- ² H. Ohno, Science **281**, 951 (1998). H. Ohno et al., Nature (London) 408, 944 (2000).
- ³ R. Fiederling *et al.*, Nature **402**, 787 (1999).
- ⁴ A. Hachè *et al.*, Phys. Rev. Lett. **78** 306 (1997). A. Gupta *et al.* Science **292** 2458 (2001). M. J. Stevens *et al.*, Phys. Rev. Lett. **90** 136603 (2003).
- ⁵ S. A. Crooker *et. al.*, PRB56, 7574 (1997). S. Koshihara *et al.*, Phys. Rev. Lett. **78**, 4617 (1997) R. Akimoto *et al.*, Phys. Rev. **B57**, 7208 (1998). A. Oiwa *et al.*, Phys. Rev. Lett. **88** 137202 (2002). J. Wang *et al.*, cond-mat-0305017. J. Bao, *et al.* , Nature Mater. **2**, 175 (2003).
- ⁶ J. K. Furdyna, J. Appl. Phys **64**, R29 (1988).
- ⁷ T. Dietl *et al.*, Science **287** 1019 (2000).
- ⁸ C. Piermarocchi *et al.* Phys. Rev. Lett. **89**, 167402 (2002).
- ⁹ S. Schmitt-Rink, D. Chemla Phys. Rev. Lett**57**, 2752 (1986). S. Schmitt-Rink, D. S. Chemla and H. Haug, Phys. Rev. **B37**, 941 (1988)
- ¹⁰ C. Comte and G. Mahler, Phys. Rev. **B38**, 10517 (1988)
- ¹¹ S. Glutsch and R. Zimmermann, Phys. Rev. **B45**, 5857 (1992)
- ¹² P. Nozieres and C. Comte, J. de Physique **43**, 1083 (1982). J. Fernandez-Rossier and C. Tejedor,

- Phys. Rev. Lett **78**, 4809 (1997)
- ¹³ J. Fernandez-Rossier and L. J. Sham Phys. Rev. B **64**, 235323 (2001)
- ¹⁴ For $\text{Zn}_{0.988}\text{Mn}_{0.012}\text{S}$ we take the exciton Bohr radius, $a_B = 21 \text{ \AA}$ and the exchange constants $J_e = 7.8 \text{ eV \AA}^3$ ($\alpha = 0.2 \text{ eV}$) and $J_h = -59.04 \text{ eV \AA}^3$ ($\beta = -1.5 \text{ eV}$).
- ¹⁵ H. Kamada *et al.* Phys. Rev. Lett. **87**, 246401 (2001)
- ¹⁶ O. D. Mücke *et al.* , Phys. Rev. Lett. **87**, 057401 (2001).
- ¹⁷ We remark that the experimental values of the Rabi energies mentioned refer to InGaAs/GaAs systems. We are not aware of direct measurements of the Rabi energies in (Zn,Mn)S. However, the dipole transition matrix elements for the two materials are comparable. See e.g. P. Lawaetz, Phys. Rev B **4**, 3460 (1971).
- ¹⁸ T. Dietl *et al.*, Phys. Rev. Lett. **74**, 474 (1995).
- ¹⁹ H. Boukari *et al.*, Phys. Rev. Lett. **88**, 207204 (2002).

CAPTION Figure 1

Energy contributions as a function of \mathcal{M} . Figure 1-A. Upper panel: $\mathcal{G}_S(\mathcal{M})$ for two different temperatures. Middle panel: $\frac{\mathcal{E}(\mathcal{M})}{V}$ for $\delta = 41$ meV and $\Omega = 5$ meV. Lower panel: $\mathcal{M}(T/T_c)$ for $\Omega = 5$ meV and three different values of δ . Figure 1-B: total Landau energy $\mathcal{G}(\mathcal{M})$ for the Mn, for a set of temperatures nearby T_c for $\delta = 41$ meV and $\Omega = 5$ meV.

CAPTION Figure 2

(A). Contour map for transition temperature as a function of the Rabi energy Ω and the detuning δ , for $(\text{Zn}_{0.99}, \text{Mn}_{0.01})\text{S}$. White region: outside validity range of linear response. (B) $\mathcal{M}(\Omega, \delta)$ at a fixed temperature, $k_B T = 0.5$ Kelvin for $\text{Zn}_{0.988}\text{Mn}_{0.012}\text{S}$. (C) Schematic $(k_B T, \delta/J_{\max})$ phase diagram, for fixed laser intensity. In the left region ($\delta < 0$) (right region ($\delta > J_{\max}$)) the system is always absorbing (coherent). The red line in the coherent side signals the ferromagnetic instability described in this work. The red line in the absorbing part corresponds to photocarrier mediated ferromagnetism $T_c^{7,19}$. The middle region shows a possible transition from a paramagnetic-coherent towards a ferromagnetic-absorbing phase.

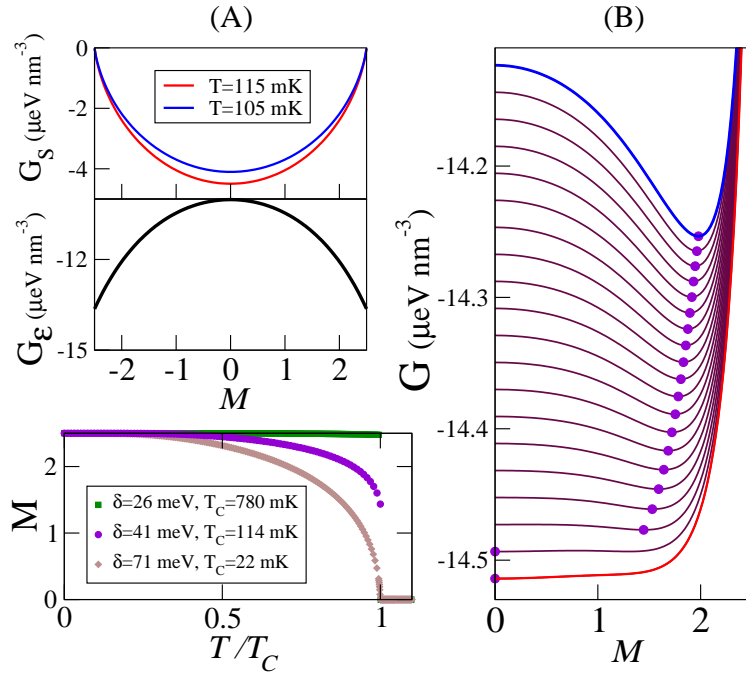


Figure 1

